

## $I=0, J^P=1^-$ Quasibound State in the $\eta NN$ - $\pi NN$ Coupled System

Tamotsu Ueda

Faculty of Engineering Science, Osaka University, Toyonaka, Osaka 560, Japan

(Received 24 September 1990)

The existence of an  $I=0, J^P=1^-$  quasibound state in the  $\eta NN$ - $\pi NN$  coupled system is theoretically predicted with a mass of about 2430 MeV and a width 10–20 MeV. The three-body equation for the  $\pi NN$ - $\pi NN$  coupled system is solved. The primary two-body interactions generating the bound state are (1) the  $NN$  interaction in the  ${}^8S_1$ - ${}^3D_1$  state and (2) the  $\pi N$  and  $\eta N$  coupled interaction in the  $S_{11}$  state. A remarkable enhancement of the elastic cross section of  $\eta$ - $d$  scattering near the  $\eta d$  threshold is found, whose origin is in the pole structure of the  $I=0, J^P=1^-$   $\eta d$  scattering amplitude on the complex energy plane.

PACS numbers: 14.20.Pt, 11.80.Jy, 13.75.-n, 25.80.Hp

The possibility of the existence of  $\pi NN$  bound states has been suggested by many people. Since strong attraction due to the  $\pi N$  interaction in the  $P_{33}$  state and the  $NN$  interaction in the  ${}^3S_1$  state exists in the system, a bound state has been expected there. However, the large centrifugal repulsion in the  $P_{33}$  resonance makes it difficult for the system to be bound. Therefore, rather than a bound state, resonance states exist in the  $\pi NN$  system.  $J^P=2^+$  and  $J^P=3^-$  resonances are theoretically predicted, in agreement with the experimental data.<sup>1</sup>

In turn, the  $\eta NN$  system has different properties from the  $\pi NN$  system. In this system the important interactions are the  $\eta N$ - $\pi N$  interaction in the  $S_{11}$  state and the  $NN$  interaction in the  ${}^3S_1$  state. Namely, both interactions are of the  $S$ -wave nature, giving no centrifugal repulsion, and providing a greater possibility for a bound  $\eta NN$  state. One motivation for this work is to explore this possibility.

Another motivation is that the interest of nuclear physicists in "GeV pion physics" beyond the  $\Delta$ -resonance region has recently been enhanced. In this context the  $\eta$ -nucleus interaction is an interesting theme. Already  $\eta$ -nucleus bound states have been discussed in the framework of the  $\eta$ -nucleus optical potential.<sup>2,3</sup> Bound states with  $A \geq 12$  are predicted.<sup>2</sup> Furthermore, pioneering experimental results have also been presented about  $\eta$ -few-nucleon systems.<sup>4,5</sup>

In nuclear many-body systems with  $A \gg 2$ , the complex nuclear-medium effects are essentially important. In contrast with this, the problem can be more exactly investigated in the  $\eta NN$  system within the framework of the three-body formalism. This paper reports results just from this three-body approach.

Since the  $S_{11}$  resonance couples both to the  $\pi N$  and  $\eta N$  channels, the  $\eta NN$  system couples necessarily to the  $\pi NN$  system. A method of treating the coupled plural three-body system has been developed by the present author and others.<sup>6-8</sup> The method has been applied to  $\pi NN$ - $\rho NN$ ,<sup>6</sup>  $NNN$ - $NN\Delta$ - $\pi dN$ ,<sup>7</sup> and other systems.<sup>8</sup>

The three-body equation for the amplitude  $X_{\alpha\beta}$  is writ-

ten as

$$X_{\alpha\beta} = Z_{\alpha\beta} + \sum_{\mu,\nu} Z_{\alpha\mu} \tau_{\mu\nu} X_{\nu\beta}, \quad (1)$$

where  $Z_{\alpha\beta}$  is the particle-rearrangement term between the particle channels  $\alpha$  and  $\beta$ , while  $\tau_{\mu\nu}$  is the propagation term of the system with a spectator particle and an interacting pair in the intermediate channel. Equation (1) is the integral equation where the variable is the relative momentum between the spectator particle and the interacting pair.  $Z$  and  $\tau$  have the standard form of three-body theory<sup>9</sup> and are about the same as those in Ref. 6. They are given by the form factors of separable input potentials and the free three-body Green functions (see Fig. 1).

In Table I the particle channels and the locations of the nonvanishing matrix elements for  $Z$  and  $\tau$  are given.

In this paper we concentrate on the  $I=0, J^P=1^-$  state of the  $\eta NN$ - $\pi NN$  coupled system. Then the angular-momentum channels as shown in Table II are taken into account. Of course, Eq. (1) could give the amplitudes for all the processes of the system. Among these we calculate the  $\eta d$  scattering amplitudes.

The input two-body interactions involve the  $\pi N$  potential in the  $P_{11}$  state, the  $NN$  potential in the  ${}^3S_1$ - ${}^3D_1$  state, and  $\pi N$ - $\eta N$  potential in the  $S_{11}$  state. One notes that the  $P_{33}$   $\pi N$  and the  ${}^1S_0$   $NN$  potentials do not work in the present three-body state for the sake of the isospin invariance.

For the  $P_{11}$   $\pi N$  potential the nucleon pole part is taken



FIG. 1. The graphical representation of the first, the second, and one of the third terms in the perturbation series due to Eq. (1) for the  $\eta d \rightarrow \eta d$  amplitude. The solid and dotted lines indicate the nucleon and the mesons, respectively, while the solid+dotted lines represent the interacting pair in the  $S_{11}$  or  $P_{11}$  state.

TABLE I. The particle channel and the locations of nonvanishing  $Z$  and  $\tau$  matrix elements. The interacting pairs in the particle channel are in parentheses.

Channel	$(N_2\pi)N_1$	$(N_1\pi)N_2$	$(N_1N_2)\pi$	$(N_2\eta)N_1$	$(N_1\eta)N_2$	$(N_1N_2)\eta$
$(N_2\pi)N_1$	$\tau$	$Z$	$Z$	$\tau$		
$(N_1\pi)N_2$	$Z$	$\tau$	$Z$		$\tau$	
$(N_1N_2)\pi$	$Z$	$Z$	$\tau$			
$(N_2\eta)N_1$	$\tau$			$\tau$	$Z$	$Z$
$(N_1\eta)N_2$		$\tau$		$Z$	$\tau$	$Z$
$(N_1N_2)\eta$				$Z$	$Z$	$\tau$

into account. So, the  $NN$  channel is involved as  $(\pi+N)_{N \text{ pole}}+N$ , namely, channel 1 in Table II. The Roper resonance is ignored. Since this resonance does not couple with the  $\eta N$  channel, the effect of the Roper resonance is negligible in the present problem. For the  ${}^3S_1$ - ${}^3D_1$   $NN$  potential one employs two potentials: One comes from the deuteron wave function due to the Ueda-Green one-boson-exchange potential<sup>10</sup> and the other from the  $n\bar{p}$  scattering data of Phillips.<sup>11</sup>

For the  $S_{11}$   $\pi N$  and  $\eta N$  interaction the potential is

$$\begin{pmatrix} V_{\pi\pi}(p,p') & V_{\pi\eta}(p,p') \\ V_{\eta\pi}(p,p') & V_{\eta\eta}(p,p') \end{pmatrix} = - \begin{pmatrix} g_\pi(p)g_\pi(p') & g_\pi(p)g_\eta(p') \\ g_\eta(p)g_\pi(p') & g_\eta(p)g_\eta(p') \end{pmatrix}, \quad (2)$$

where  $p$  and  $p'$  are the magnitudes of the final and initial relative momenta, respectively. The form factors have the parametrization

$$g_\pi(p) = \frac{C_\pi}{p^2 + \beta_\pi^2}, \quad (3)$$

$$g_\eta(p) = \frac{C_\eta}{p^2 + \beta_\eta^2} \left[ 1 + a \left( \frac{p^2}{p^2 + \beta_\eta^2} \right)^{1/2} \right]. \quad (4)$$

Two sets of the parameters are obtained: One is made by fitting the  $\pi N$  scattering amplitude derived in the analysis by Arndt, Ford, and Roper<sup>12</sup> and the other by fitting that from the Karlsruhe-Helsinki group.<sup>13</sup> Both sets are fitted to the respective amplitudes up to the incident pion energy  $T_\pi \leq 670$  MeV, or  $\sqrt{s} \leq 1556$  MeV, the energy region where the  $S_{11}$  resonance ( $\sqrt{s} = 1535$

TABLE II. The angular-momentum channels for the  $I=0$ ,  $J^P=1^-$  state. The heading second row indicates the quantum numbers of the interacting pair.  $S_3$  and  $L_3$  represent the total spin and the orbital angular momentum, respectively, possessed by the interacting pair and the spectator.

Channel No.	1	2	3	4	5
	$P_{11}$	$S_{11}$	$S_{11}$	${}^3S_1$ - ${}^3D_1$	${}^3S_1$ - ${}^3D_1$
$S_3$	0	1	1	1	1
$L_3$	1	0	2	0	2

MeV) is fully involved (see Fig. 2). The parameter values for the  $S_{11}$  potential are as follows:  $C_\pi=0.7$   $\text{fm}^{-1}$ ,  $\beta_\pi=440$  MeV,  $C_\eta=10.0$   $\text{fm}^{-1}$ ,  $\beta_1=\beta_2=1900$  MeV in common for sets I and II, while  $a=1.02$  and  $1.05$  for sets I and II, respectively.

The  $S_{11}$  resonance couples to the  $\pi N$ ,  $\eta N$ , and  $\pi\pi N$  channels with branching ratios of 50:45:10 to 35:55:10.<sup>14</sup> The present two-channel parametrization yields the  $\pi N$ - $\pi N$  and  $\pi N$ - $\eta N$  cross sections in the ratio of 50:43 at  $\sqrt{s}=1510$  MeV and 35:51 at  $\sqrt{s}=1541$  MeV, in approximate agreement with the experimental data. On the other hand, the total cross section due to set II is larger than that due to set I by about 10%. Therefore the error due to the neglect of the  $\pi\pi N$  channel in the present parametrization can be estimated by observing the difference between the two results of the three-body calculations when sets I and II are used.

I set up three models for the three-body calculation: Models I and II employ set I and II parametrizations for the  $S_{11}$  potential, respectively, while both models use the Ueda-Green interaction for the  ${}^3S_1$ - ${}^3D_1$  potential. Model III employs set I for the  $S_{11}$  potential and the Phillips parametrization for the  ${}^3S_1$ - ${}^3D_1$  potential.

The results for the  $\eta d$  scattering amplitudes of the  $I=0$ ,  $J^P=1^-$  state are displayed in Fig. 3. The Argand

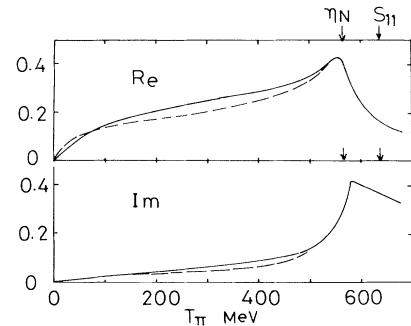


FIG. 2. The  $\pi N$  amplitudes by set I parametrization and by Arndt, Ford, and Roper (Ref. 12) are represented by the solid and dashed curves, respectively. The upper and lower parts show the real and imaginary parts of the amplitudes, respectively. The arrows represent the thresholds. The abscissa represents the incident-pion kinetic energy in the laboratory system.

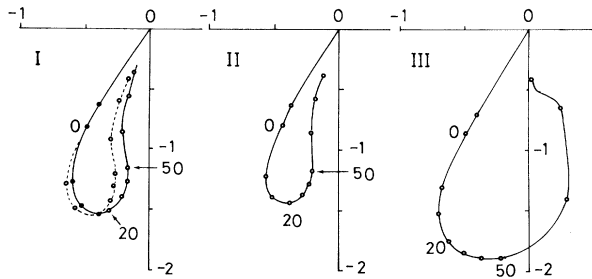


FIG. 3. (I) The Argand plots of the model I amplitude. The solid and dashed curves indicate the cases with channels 2 and 4 and channels 2, 3, and 4, respectively. (II), (III) The model II and III amplitudes are represented by the solid curves. Both employ channels 2 and 4. The circles indicate the energy points  $E_\eta = -1, 0, 5, 10, 20, 30, 40, 50, 100, 200,$  and  $300$  MeV. The  $S_{11}$   $N$  threshold is at  $E_\eta = 45$  MeV for the  $S_{11}$  mass  $1535$  MeV.

plots of the  $T$ -matrix amplitudes are shown as a function of the energy  $E_\eta$ . The  $T$  matrix is obtained by multiplying the matrix  $X_{\alpha\beta}$  for the initial and final  $\eta d$  channels by the magnitude of the  $\eta d$  relative momentum and is related to the  $S$  matrix by  $S = 1 - iT$ . The energy variable  $E_\eta$  represents the total energy minus the  $\eta NN$  threshold energy  $2430$  MeV. The  $\eta$ - $d$  threshold locates at  $E_\eta = -2.225$  MeV, namely, the negative of the deuteron binding energy.

First, the contributions of each channel to the amplitudes are explained. The important contributions come from channels 2 and 4 in Table II. These two channels make the major contribution to the characteristic feature of the amplitudes. The contribution of channel 3 is appreciable as is seen in the comparison of the cases with and without channel 3 in Fig. 3 (I). Furthermore, the contributions of channels 1 and 5 have been confirmed to be very small. Therefore, the results of the calculations with just channels 2 and 4 or channels 2, 3, and 4 are displayed in Fig. 3.

The  $\eta d$  scattering amplitudes of the  $I=0, J^P=1^-$  state have a very surprising feature in the energy region from the  $\eta NN$  threshold ( $E_\eta=0$ ) through the  $S_{11}$ -resonance production energy ( $E_\eta \approx 45$  MeV). The Argand plots of the amplitudes of the three models all indicate anticlockwise looping behavior. This suggests the existence of a resonance or bound state of the  $\eta NN$ - $\pi NN$  system. This looping behavior is common to all three models, irrespective of the two-body input interactions for the  ${}^3S_1$ - ${}^3D_1$  as well as the  $S_{11}$  channels. One also understands that the neglect of the  $\pi\pi N$  channel in the  $\pi N$ - $\eta N$  potential does not matter to the looping behavior in the comparison of the two results from models I and II.

The analytic structure of the amplitude of model III on the complex energy plane has been investigated. A pole structure is observed near the  $\eta d$  threshold on the

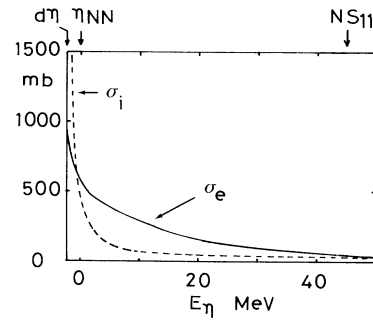


FIG. 4. The elastic and inelastic cross sections for  $\eta d$  scattering due to model I with channels 2 and 4 are indicated by the solid and the dashed curves, respectively. The arrows indicate the thresholds.

second Riemann sheet with respect to the  $\eta NN$  and  $\eta d$  cuts. The real part of the pole position is  $\text{Re}E_\eta \approx -2.0$  MeV, or a little less than this value, and the imaginary part is  $\text{Im}E_\eta \approx -10$  MeV. A similar pole structure is also inferred for the amplitudes of models I and II, since the behavior of these is similar to that of model III on the real energies.

Figure 4 shows the elastic and inelastic cross sections for  $\eta$ - $d$  scattering. One notes the strong enhancement of the elastic cross section at  $E_\eta = -2.225$  MeV. This should tend to a constant when  $E_\eta \rightarrow -2.225$  MeV. On the other hand, the inelastic cross section has a behavior like  $p^{-1}$ , where  $p$  is the magnitude of the relative momentum between  $\eta$  and  $d$ . Observing the shape of the enhanced elastic cross section and also taking into account the pole position, one judges that the quasibound state is located at about  $\sqrt{s} = 2430$  MeV with a width of  $10$ - $20$  MeV. The decay width to  $NN$  is much smaller than this, since the effect of channel 1, the  ${}^1P_1 NN$  channel, is very small. The matrix element for a transition to channel 1 by pion rearrangement is small due to its  $P$ -wave form factor and relatively large energy denominator.

One obtains the scattering lengths as

$$a = -1.69 - 2.20i, \quad -1.11 - 2.91i, \quad -1.84 - 2.47i, \quad (5)$$

in units of fm for models I, II, and III, respectively.

I remark here that the most important origin for binding of the  $\eta NN$ - $\pi NN$  system arises from the mechanism of nucleon rearrangement with  $S_{11}$   $\eta N$ , and  ${}^3S_1$   $NN$  interactions in the initial and final two-body channels. The  $Z$  term for this mechanism becomes very large at the  $\eta NN$  threshold, since the energy denominator becomes very small, while the numerator factors  $g_\eta(p)$  of the  $S$  waves are large there.

The present result of the existence of a quasibound state in the  $\eta NN$ - $\pi NN$  system is rather surprising from the viewpoint of the optical-potential approach to the

$A \gg 2$  systems, where  $A \geq 12$  is the condition for the existence of bound states.<sup>2</sup> However, this bound-state condition is not valid for the  $\eta$ -few-nucleon system. Furthermore, in the  $A \gg 2$  systems  $S_{11} \rightarrow \eta N$  vertex effects are suppressed by the Pauli blocking effect.<sup>3</sup> However, this vertex makes very important contributions to the quasibound state of the  $\eta NN$ - $\pi NN$  system. Thus the bound-state problem for the  $\eta$ -few-nucleon system is beyond the scope of the optical-potential approach.

The present result cannot be reached from any low-order perturbation calculation. The fifth-order term is still in the same order of magnitude as the first. Even the eleventh is about one-tenth of the first.

Since one observes a pole structure associated with the enhancement of the amplitude at  $\eta d$  threshold, the amplitudes for all the processes of the system should have an enhancement there. Therefore the quasibound state can be investigated experimentally through the reactions  $\gamma d \rightarrow \eta d$  ( $T_\gamma = 633$  MeV),  $np \rightarrow \eta d$  ( $T_p = 1260$  MeV),  $\pi d \rightarrow (\eta d)\pi$  ( $T_\pi = 590$  MeV),  $np \rightarrow np$  ( $T_n = 1260$  MeV),  $pd \rightarrow (\eta d)p$  ( $T_d = 1800$  MeV), etc., where the energies in parentheses indicate the incident kinetic energies in the laboratory system.

Finally, I remark about the result when an  $S_{11}$   $\eta N$  potential with resonance energy about 10 MeV deeper than that of set I is used. In this case the resulting  $\eta d$  scattering amplitude has a clockwise looping behavior. Then the  $\eta d$  phase shift begins from  $180^\circ$  at the  $\eta d$  threshold and goes down with increasing energy. The pole is found at  $E_\eta = 1.27 - 0.90i$  MeV in the first and second Riemann sheets with respect to the  $\eta d$  and  $\eta NN$  cuts, re-

spectively.<sup>15</sup>

In conclusion, I find an  $I=0$ ,  $J^P=1^-$  quasibound state near the  $\eta d$  threshold ( $\sqrt{s} = 2430$  MeV) with a width of about 10–20 MeV in a calculation of the coupled  $\eta NN$ - $\pi NN$  system.

<sup>1</sup>T. Ueda, Nucl. Phys. **A463**, 69c (1987).

<sup>2</sup>Q. Haider and L. C. Liu, Phys. Lett. **172B**, 257 (1986).

<sup>3</sup>M. Kohno and H. Tanabe, Phys. Lett. **B 231**, 219 (1989).

<sup>4</sup>F. Plouin, P. Fleury, and C. Wilkin, Phys. Rev. Lett. **65**, 690 (1990).

<sup>5</sup>J. C. Peng *et al.*, Phys. Rev. Lett. **63**, 2353 (1989); J. Berger *et al.*, Phys. Rev. Lett. **61**, 919 (1988).

<sup>6</sup>T. Ueda, Phys. Lett. **141B**, 157 (1984).

<sup>7</sup>T. Ueda, Nucl. Phys. **A505**, 610 (1989).

<sup>8</sup>K. Miyagawa, T. Ueda, T. Sawada, and S. Takagi, Nucl. Phys. **A459**, 93 (1986).

<sup>9</sup>E. O. Alt, P. Grassberger, and W. Sandhas, Nucl. Phys. **A139**, 209 (1969); Y. Avishai and T. Mizutani, Nucl. Phys. **A326**, 352 (1979); I. R. Afnan and B. Blankleider, Phys. Rev. **C 22**, 1638 (1980).

<sup>10</sup>T. Ueda and A. E. S. Green, Phys. Rev. **174**, 1304 (1968).

<sup>11</sup>A. C. Phillips, Nucl. Phys. **A107**, 209 (1968).

<sup>12</sup>R. A. Arndt, J. M. Ford, and L. D. Roper, Phys. Rev. **D 32**, 1085 (1985).

<sup>13</sup>R. Koch and E. Pietarinen, Nucl. Phys. **A336**, 331 (1980).

<sup>14</sup>Particle Data Group, G. P. Yost *et al.*, Phys. Lett. **B 204**, 1 (1988).

<sup>15</sup>T. Ueda, in Proceedings of 1990 Topical Conference on Particle Production Near Threshold, Nashville, Indiana, 1990 (to be published).